Supporting Information

Rational Design of a Reversible Mg^{2+}/EDTA-controlled Molecular Switch Based on a DNA Minidumbbell

Liqi Wan,[b] Sik Lok Lam,*[b†] Hung Kay Lee [b] and Pei Guo *[a]

[a] School of Biology and Biological Engineering, South China University of Technology, Guangzhou, Guangdong 510006, China

[b] Department of Chemistry, The Chinese University of Hong Kong, Shatin, New Territories, Hong Kong SAR, China

Corresponding Authors

*[a] E-mail: peiguo@scut.edu.cn

*[b†] E-mail: lams@cuhk.edu.hk

Materials and Methods

DNA samples. The DNA samples were synthesized on an Applied Biosystems model 394 DNA synthesizer, purified with denaturing polyacrylamide gel electrophoresis and diethylaminoethyl Sephacel anion exchange column chromatography and desalted using Amicon Ultra-4 centrifugal filtering devices. The NMR samples were prepared by dissolving ~0.25 μmol DNA samples in 500 μL buffer containing 0.02 mM 2,2-dimethyl-2-silapentane-5-sulfonic acid (DSS) and 10 mM sodium phosphate (pH 7.0).

NMR experiments. All NMR experiments were performed on a Bruker AVANCE-500 and/or AVANCE-700 MHz NMR spectrometer. For studying labile proton signals, the sample was dissolved in a 90% H_2O/ 10% D_2O buffer solution. One-dimensional (1D) proton spectra and two-dimensional (2D) nuclear Overhauser effect spectroscopy (NOESY) were acquired using the excitation sculpting[1] or jump-return[2] pulse sequence to suppress the water signal. For studying non-labile proton signals, 99.96% D_2O solvent was used and a 2-s presaturation pulse was applied to suppress the residual water signal. The 2D double-quantum-filtered correlation spectroscopy (DQF-COSY) experiments were performed to measure the $^3J_{H1'H2'}$, $^3J_{H4'H5'}$ and $^3J_{H4'H5''}$ coupling constants. A mixing time of 75 ms was used for 2D total correlation spectroscopy (TOCSY) experiments. Data sets of 4096 × 512 were acquired for NOESY, COSY and TOCSY experiments. ^{1}H-^{13}C heteronuclear multiple bond correlation (HMBC) experiments were carried out with an evolution period of 65 ms for adenine H2 assignments.[3] ^{31}P signals were assigned by ^{1}H-^{31}P heteronuclear single-quantum coherence (HSQC) experiments conducted with a data size of 4096 × 200. In the HSQC experiments, a Carr-Purcell-Meiboom-Gill (CPMG) pulse train was employed during the periods of magnetization transfer between phosphorus and scalar coupled proton nuclei,[4] and the delays surrounding synchronous proton/phosphorus 180°

refocusing pulses were set to be ~100 μs. ^{13}C and ^{31}P chemical shifts were indirectly referenced to DSS signal using the derived nucleus-specific ratios of 0.251449530 and 0.404808636, respectively.[5]

NMR assignments. Sequential resonance assignments of CTTG_X, CCTG_X and TTTA_X were accomplished from the H6/H8-H1' fingerprint regions using standard methods,[6] and they are shown in Figures S8-10. H2' and H2'' signals were assigned based on correlations with intranucleotide H1' in the DQF-COSY spectra, and they were distinguished by comparing the relative intensities of intranucleotide H1'-H2' and H1'-H2'' NOEs.[7,8] H3' signals were assigned based on correlations with intranucleotide H1'/H2'/H2'' in the TOCSY spectra. H4' signals were assigned by correlations with intranucleotide H3' in the DQF-COSY spectra. H5' and H5'' stereospecific assignments were achieved by analyzing the $^{3}J_{H4'-H5'}$ and $^{3}J_{H4'-H5''}$ coupling constants, and the relative intensities of intranucleotide H3'-H5'/H5'' NOEs.[6] For the abasic site residue, the two protons attached to the C1' atom were named as H1'1 and H1'2, and they were differentiated by stronger intranucleotide H1'1-H2'' NOE than H1'2-H2'' NOE.[8] Adenine H2 assignments were confirmed by ^{1}H-^{13}C HMBC experiments with both H2 and H8 showed couplings to C4.[3] The guanine H1 signals in C-G Watson-Crick base pairs were assigned based on their NOEs with cytosine H41/H42. ^{31}P signals were assigned based on the correlation between the H3' resonance of the i^{th} residue and the ^{31}P resonance of the $(i+1)^{th}$ residue in ^{1}H-^{31}P HSQC spectra (Figures S11-13). The ^{1}H and ^{31}P chemical shifts of the CTTG_X, CCTG_X and TTTA_X MDB are summarized in Tables S4, S5 and S6, respectively.

Optical melting experiments. Ultraviolet (UV) melting experiments were performed to determine the thermodynamic stabilities of the CTTG_X, CCTG_X and TTTA_X MDBs, and the previously reported CTTG, CCTG and TTTA MDBs.[9-11] The concentrations of DNA

samples were kept at 2~5 μM in the NMR buffer solution, and a 10 mm path length cuvette was used. UV absorbances at 260 nm were collected using a Hewlett-Packard 8453 diode-array UV-visible spectrophotometer. The UV absorbances were monitored from 10 to 80 °C for the CTTG_X MDB, 10 to 75 °C for the CCTG_X and TTTA_X MDBs, 10 to 70 °C for the CTTG MDB, and 10 to 50 °C for the CCTG and TTTA MDBs, with a heating rate of 1.0 °C/min. A nitrogen gas surge was supplied at temperatures below 15 °C to avoid water condensation on the cuvette. The sample temperatures were monitored by putting a BetaTHERM thermistor temperature sensor into the samples. Three replicative measurements were carried out for each sequence. The T_m and ΔG° values were extracted by fitting the melting curves with a two-state transition model.[12]

NMR experimental restraints. Solution structures of the CTTG_X and CCTG_X MDBs were calculated with NMR experimental restraints. Proton-proton distance restraints were extracted from the 2D NOESY spectra acquired at a mixing time of 200 ms at 0 °C for the CTTG_X MDB and 300 ms for the CCTG_X MDB. We divided NOE cross peaks into five categories based on their intensities, including strong, strong or medium, medium, medium or weak, and weak. Distance ranges of 1.8-4.0, 2.5-4.5, 3.0-5.0, 3.5-5.5 and 4.0-6.2 Å were applied to these categories, respectively. Distance restraints for hydrogen bonds in Watson-Crick C-G base pairs were also used.[13] The H1'-C1'-C2'-H2' dihedral angles were determined by the $^3J_{H1'H2'}$ coupling constants measured from the DQF-COSY spectra using the Karplus equation.[14] Glycosidic torsion angles χ were obtained by the analysis of intranucleotide H6/8-H1' NOE cross peaks in the NOESY spectra. Backbone torsion angles γ were determined based on the analysis of $^3J_{H4'-H5'}$ and $^3J_{H4'-H5''}$ coupling constants.[6] The chirality of deoxyribose carbons were restrained by improper torsions. For natural nucleotides, the chirality restraints were generated

by AMBER16.[15] For the abasic site residue, we manually added the same chirality restraints. All the experimental restraints used for calculating solution structures of the CTTG_X and CCTG_X MDBs are summarized in Tables S2 and S3, respectively.

Modification of AMBER force field for the abasic site. We modified the force field parameters for the abasic site by using DT (thymine) as a template, removed the base protons from DT, and then added H1'2 to the deoxyribose C1', and the original H1' attached to C1' was renamed to be H1'1. Notably, following the rules of DNA residue names in AMBER force field (two capital letters for non-terminal residues), we set the residue name of the abasic site to be "DX" in the modified AMBER force field but not "X" represented in the main text. We made use of the previously reported partial charge assignments for DX,[16] and the velocity and angle for the OS-CT-HC (O4'-C1'-H1') bond of DX were set to be 50 $kcal \cdot mol^{-1} \cdot rad^{-2}$ and 106.8°, respectively.[17] Other force field parameters of DX, such as the atom names and atom types, were assigned to be consistent with those of the natural nucleotides.

Structure calculations. Restrained molecular dynamics (rMD) calculations of the CTTG_X and CCTG_X MDBs were performed using AMBER16 with OL15 force field.[15,18] The initial single-strand structures of 5'-CTTG(DX)CTTG3' and 5'-CCTG(DX)CCTG-3' were obtained by replacing the T5 residue in sequences 5'-CTTGTCTTG-3' and 5'-CCTGTCCTG-3' with a DX residue, respectively. The cutoff value for nonbonded interactions was set to be 9.0 Å. Eight sodium ions were added to the single strand to neutralize backbone charges. For the CTTG_X MDB, *in vacuo* calculations were initiated by heating the system from 300 K to 800 K in the first 3 ps, and then maintaining at 800 K for 10 ps, followed by cooling to 300 K from 13 to 30 ps. After 5 ps equilibration at 300 K, the structural coordinates were subjected to restrained energy minimization (rEM) by 200 steps of steepest descent, and then conjugate gradient until the

energy gradient difference between successive minimization steps was smaller than 0.1 kcal/mol·Å^2. For the CCTG_X MDB, the system was heated up to 2000 K in the first 5 ps, and then maintained at this temperature for 15 ps. The temperature was lowered to 300 K in the following 15 ps, and then maintained at 300 K for 5 ps, followed by the same rEM process mentioned above. For both CTTG_X and CCTG_X MDBs, a total of 500 independent rMD-rEM calculations were performed with random starting velocities (random seeds), and 20 structures with the lowest total energies were selected to be representative ensembles of refined structures. NMR refinement statistics of the CTTG_X and CCTG_X MDBs are summarized in Table S1.

Structural analyses. The CPPTRAJ[19] and *suppose* modules of AMBER16 were used for statistical analyses, such as the base pair parameters and RMSD values. UCSF Chimera[20] was employed for plotting 3D structures. The presence of a hydrogen bond is defined if the distance between hydrogen bond donor and acceptor is smaller than 3.2 Å and the hydrogen bond angle is larger than 90°. Hydrophobic interactions are considered to present when the distance between two hydrocarbon moieties falls into the range of 3.8-6.5 Å.[21]

Circular dichroism (CD) experiments. CD experiments were performed on a Chirascan V100 CD spectrometer at room temperature. The samples were prepared in 1 mM sodium phosphate (NaPi) buffer solution with a DNA concentration of 20 μM, and placed in a cuvette of 10 mm path length. CD spectra were collected from 200 to 350 nm with a step size of 1 nm. CD spectra were background corrected using a 1 mM NaPi buffer solution.

Table S1. NMR refinement statistics of the CTTG_X and CCTG_X MDBs.

	CTTG_X	CCTG_X
Number of distance restraints		
Intra-residue	178	148
Inter-residue	139	145
Hydrogen bond	6	6
Subtotal	323	299
Number of torsion angle restraints		
Chirality	45	45
Glycosidic torsion (χ)	8	8
Sugar (H1'-C1'-C2'-H2')	7	7
Backbone (γ)	2	6
Subtotal	62	66
Restraint satisfaction		
Number of distance restraint violation > 0.2 Å	0	0
Number of torsion angle restraint violation > 1°	0	1
Deviation from covalent geometry		
Bonds (Å)	0.0094 ± 0.0002	0.0094 ± 0.0002
Angles (°)	2.39 ± 0.06	2.30 ± 0.08
Heavy atomic RMSD (Å)[a]		
Average pairwise RMSD	0.5 ± 0.1	0.6 ± 0.2
RMSD from mean structure	0.3 ± 0.1	0.4 ± 0.1

[a]RMSD values were calculated among 20 refined structures with the lowest total energies.

Table S2. NMR restraints for calculating solution structures of the CTTG_X MDB.

Distribution of NOE-derived distance restraints (intranucleotide/internucleotide = 178/139)

Residue	C1	T2	T3	G4	X5	C6	T7	T8	G9
C1	19	22	10	-	-	-	-	-	16
T2		25	18	2	-	-	1	-	4
T3			26	10	-	-	-	-	-
G4				13	5	5	4	-	-
X5					11	5	-	-	-
C6						19	12	8	-
T7							20	9	-
T8								21	8
G9									24

Hydrogen bond restraints

Atom pair	Distance (Å)
C1 N4-G4 O6, C6 N4-G9 O6	2.81-3.01
C1 N3-G4 N1, C6 N3-G9 N1	2.85-3.05
C1 O2-G4 N2, C6 O2-G9 N2	2.76-2.96

Sugar, backbone and glycosidic torsion angle restraints

Residue	$^3J_{H1'H2'}$ (Hz)	H1'-C1'-C2'-H2' torsion angle (°)	$^3J_{H4'H5'}$ (Hz)	$^3J_{H4'H5''}$ (Hz)	γ (°)	χ (°)
C1	9.0	139-169	[a]	[a]	-	90-270
T2	9.3	141-171	[a]	[c]	-	90-270
T3	9.6	144-174	3.8	[c]	-	90-270
G4	[a]	-	3.7	9.5	150-210 (*trans*)	90-330
X5	[b]	-	[c]	[a]	-	-
C6	9.5	143-173	[a]	[a]	-	90-270
T7	9.4	142-172	[a]	[c]	-	90-270
T8	9.6	144-174	[a]	[a]	-	90-270
G9	3.7	109-139	5.1	9.5	150-210 (*trans*)	90-330

[a]The coupling constants were not measured due to peak overlaps.
[b]The coupling constant was not measured due to a complicated coupling pattern.
[c]The coupling constants were not measured due to weak couplings.

Table S3. NMR restraints in calculating solution structures of the CCTG_X MDB.

Distribution of NOE-derived distance restraints (intranucleotide/internucleotide = 148/145)

Residue	C1	T2	T3	G4	X5	C6	T7	T8	G9
C1	24	20	10	-	-	-	-	-	20
C2		24	12	-	-	-	-	-	1
T3			16	9	-	-	-	-	-
G4				14	9	17	1	-	-
X5					6	5	-	-	-
C6						15	15	8	-
C7							17	13	-
T8								13	5
G9									19

Hydrogen bond restraints

Atom pair	Distance (Å)
C1 N4-G4 O6, C6 N4-G9 O6	2.81-3.01
C1 N3-G4 N1, C6 N3-G9 N1	2.85-3.05
C1 O2-G4 N2, C6 O2-G9 N2	2.76-2.96

Sugar, backbone and glycosidic torsion angle restraints

Residue	$^3J_{H1'H2'}$ (Hz)	H1'-C1'-C2'-H2' torsion angle (°)	$^3J_{H4'H5'}$ (Hz)	$^3J_{H4'H5''}$ (Hz)	γ (°)	χ (°)
C1	9.6	144-174	[a]	[a]	-	90-270
C2	9.8	145-175	[a]	[c]	30-90 (*gauche*+)	90-270
T3	9.9	146-176	[d]	[c]	30-90 (*gauche*+)	90-270
G4	[a]	-	3.3	9.6	150-210 (*trans*)	90-330
X5	[b]	-	5.4	9.4	150-210 (*trans*)	-
C6	10.2	149-179	[a]	[a]	-	90-270
C7	9.5	143-173	[d]	[c]	30-90 (*gauche*+)	90-270
T8	9.7	145-175	[c]	[c]	-	90-270
G9	3.6	109-139	3.9	9.5	150-210 (*trans*)	90-330

[a]The coupling constants were not measured due to peak overlaps.
[b]The coupling constant was not measured due to a complicated coupling pattern.
[c]The coupling constants were not measured due to weak couplings.
[d]The coupling constants were not measured due to peak broadenings.

Table S4. ^{1}H and ^{31}P chemical shifts (ppm) of the CTTG_X MDB at 0 °C.

Residue	H1/ H3	NH_2[a]	H6/H8 /H1'2	H5/ H7	H1'/ H1'1	H2'	H2''	H3'	H4'	H5'	H5''	^{31}P
C1	-	8.46/6.85	7.56	5.49	6.04	1.89	2.52	4.80	4.38	3.88	3.88	-
T2	11.83	-	7.98	2.04	6.55	2.25	2.44	4.86	4.44	4.25	4.16	-2.88
T3	10.97	-	7.77	1.41	5.63	1.86	2.13	4.70	3.82	3.98	4.10	-5.72
G4	13.24	9.02/5.74	7.84	-	6.04	2.85	2.85	5.00	4.28	4.04	3.61	-4.70
X5[b]	-	-	4.14	-	4.08	2.30	2.21	4.63	4.18	4.07	3.90	-3.65
C6	-	8.42/6.90	7.44	5.52	6.12	1.90	2.41	4.92	4.52	4.11	4.13	-3.90
T7	11.74	-	8.03	2.08	6.55	2.15	2.40	4.88	4.45	4.29	4.16	-2.88
T8	10.95	-	7.74	1.37	5.58	1.85	2.13	4.71	3.92	3.96	4.12	-5.96
G9	13.22	9.03/5.71	7.81	-	5.98	2.87	2.61	4.64	4.12	4.00	3.56	-4.65

[a]The amino protons in cytosine and guanine are H41/H42 and H21/H22, respectively.
[b]For X5, the two proton atoms attached to C1' atom were named as H1'1 and H1'2, respectively.

Table S5. ^{1}H and ^{31}P chemical shifts (ppm) of the CCTG_X MDB at 0 °C.

Residue	H1/ H3	NH_2[a]	H6/H8 /H1'2	H5/ H7	H1'/ H1'1	H2'	H2''	H3'	H4'	H5'	H5''	^{31}P
C1	-	8.45/6.83	7.58	5.53	6.07	1.93	2.40	4.76	4.32	3.88	3.88	-
C2	-	[b]	8.19	6.23	6.50	2.11	2.53	4.85	4.46	4.26	4.11	-2.80
T3	10.98	-	7.71	1.40	5.63	1.86	2.14	4.69	3.80	3.95	4.09	-5.65
G4	13.24	8.93/5.82	7.82	-	6.02	2.86	2.86	5.02	4.30	4.06	3.61	-4.72
X5[c]	-	-	4.14	-	4.07	2.29	2.19	4.67	4.19	4.06	3.92	-3.52
C6	-	8.37/6.89	7.46	5.57	6.13	1.94	2.32	4.88	4.48	4.11	4.14	-3.79
C7	-	[b]	8.25	6.27	6.51	2.09	2.52	4.88	4.48	4.30	4.12	-2.83
T8	10.98	-	7.67	1.37	5.59	1.87	2.13	4.69	3.87	3.94	4.09	-5.75
G9	13.25	8.93/5.95	7.80	-	5.96	2.86	2.63	4.67	4.12	3.99	3.57	-4.62

[a]The amino protons in cytosine and guanine are H41/H42 and H21/H22, respectively.
[b]The signals were too broad to be observed.
[c]For X5, the two proton atoms attached to C1' atom were named as H1'1 and H1'2, respectively.

Table S6. ^{1}H and ^{31}P chemical shifts (ppm) of the TTTA_X MDB at 15 ºC.

Residue	H3	H61/ H62	H6/H8 /H1'2	H2/ H7	H1'/ H1''1	H2'	H2''	H3'	H4'	H5'	H5''	^{31}P
T1	13.51	-	7.30	1.22	6.34	1.99	2.61	4.86	4.43	3.93	3.93	-
T2	10.40	-	7.82	2.00	6.48	2.37	2.80	4.80	4.38	[a]	[a]	-3.15
T3	[a]	-	7.55	1.59	5.65	1.79	2.04	4.61	[a]	[a]	[a]	-4.30
A4	-	[b]	8.15	8.27	6.24	3.21	2.93	5.73	4.26	4.08	3.75	-4.20
X5[c]	-	-	4.12	-	4.02	2.32	2.17	4.61	4.25	[a]	[a]	-2.90
T6	13.96	-	7.25	1.38	5.94	2.15	1.93	4.93	4.56	4.06	4.16	-4.22
T7	[a]	-	8.00	2.10	6.30	1.91	2.41	4.84	4.51	4.37	4.13	-2.95
T8	[a]	-	7.42	1.41	5.29	1.75	1.98	4.57	3.65	3.84	3.94	-5.31
A9	-	[b]	8.32	8.22	6.46	3.07	2.80	4.78	4.25	[a]	[a]	-4.35

[a]The signals were not assigned due to peak overlaps.
[b]The signals were too broad to be observed.
[c]For X5, the two proton atoms attached to C1' atom were named as H1'1 and H1'2, respectively.

Figure S1. (A) The major groove view of 20 superimposed NMR solution structures of the CTTG MDB (PDB ID: 6J37).[22] (B) The 20 individual structures showing buckled T2·T6 mispairs.

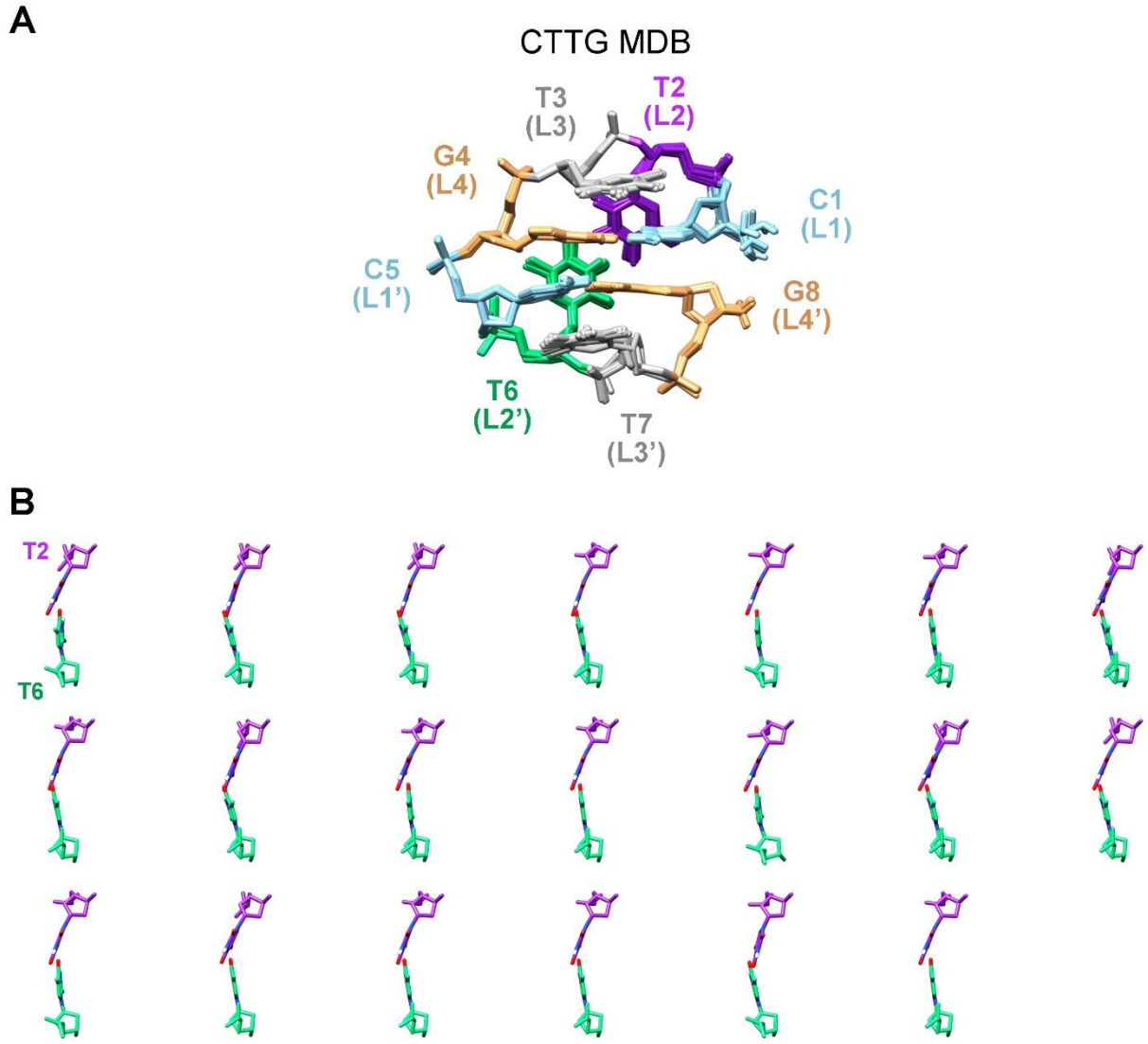

Figure S2. (A) The major groove view of 20 superimposed NMR solution structures of the CCTG MDB (PDB ID: 5GWL).[23] (B) The 20 individual structures showing exchangeable C2·C6 mispairing geometries, including (i) 13 structures showing one hydrogen bond and Na^+-mediated electrostatic interactions, (ii) 4 structures showing one hydrogen bond, (iii) 2 structures showing Na^+-mediated electrostatic interactions, and (iv) 1 structure showing two hydrogen bonds.

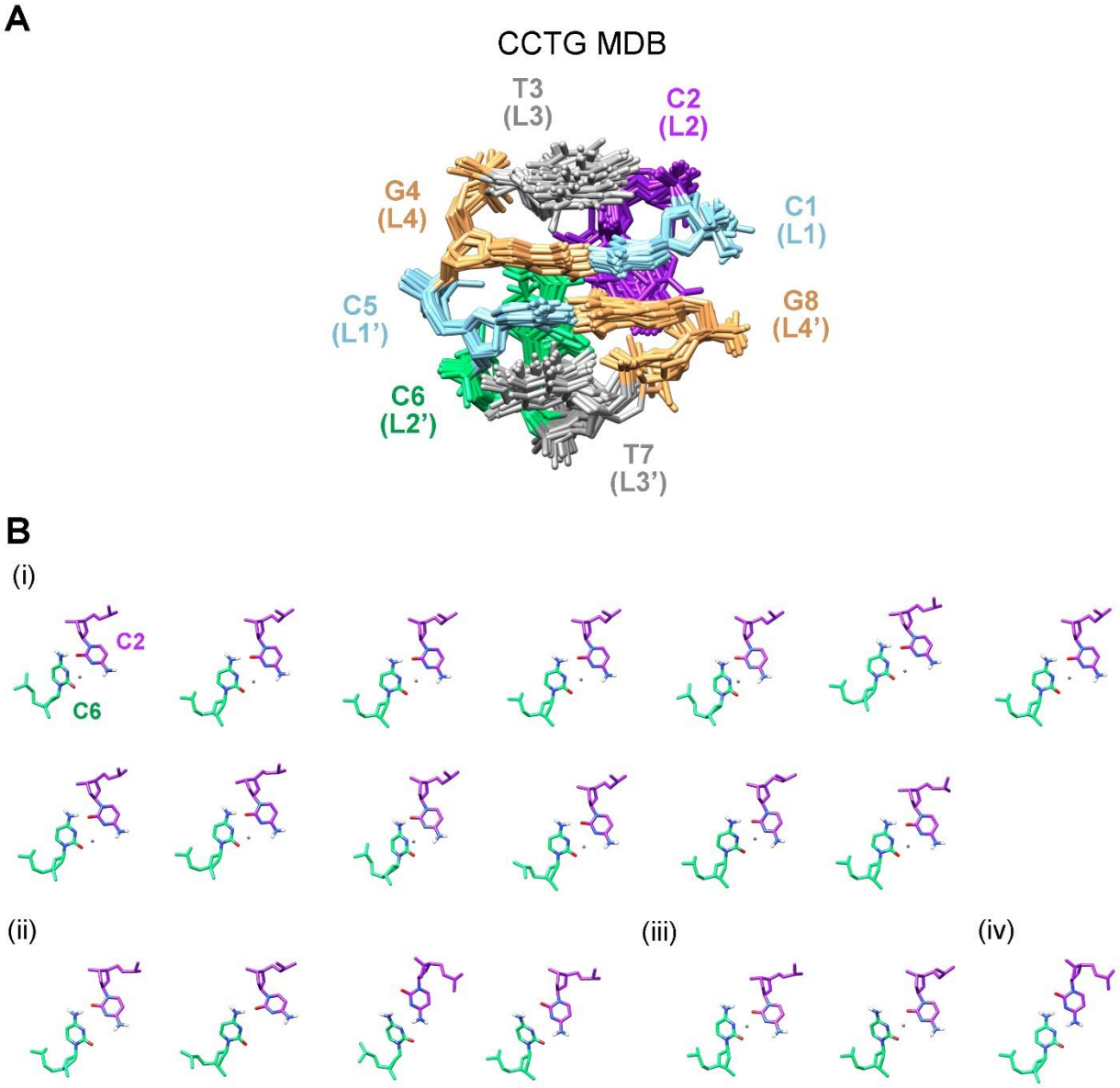

Figure S3. (A) The major groove view of 20 superimposed NMR solution structures of the TTTA MDB (PDB ID: 5GWQ).[23] (B) The 20 individual structures showing base-base stackings between T2 and T6.

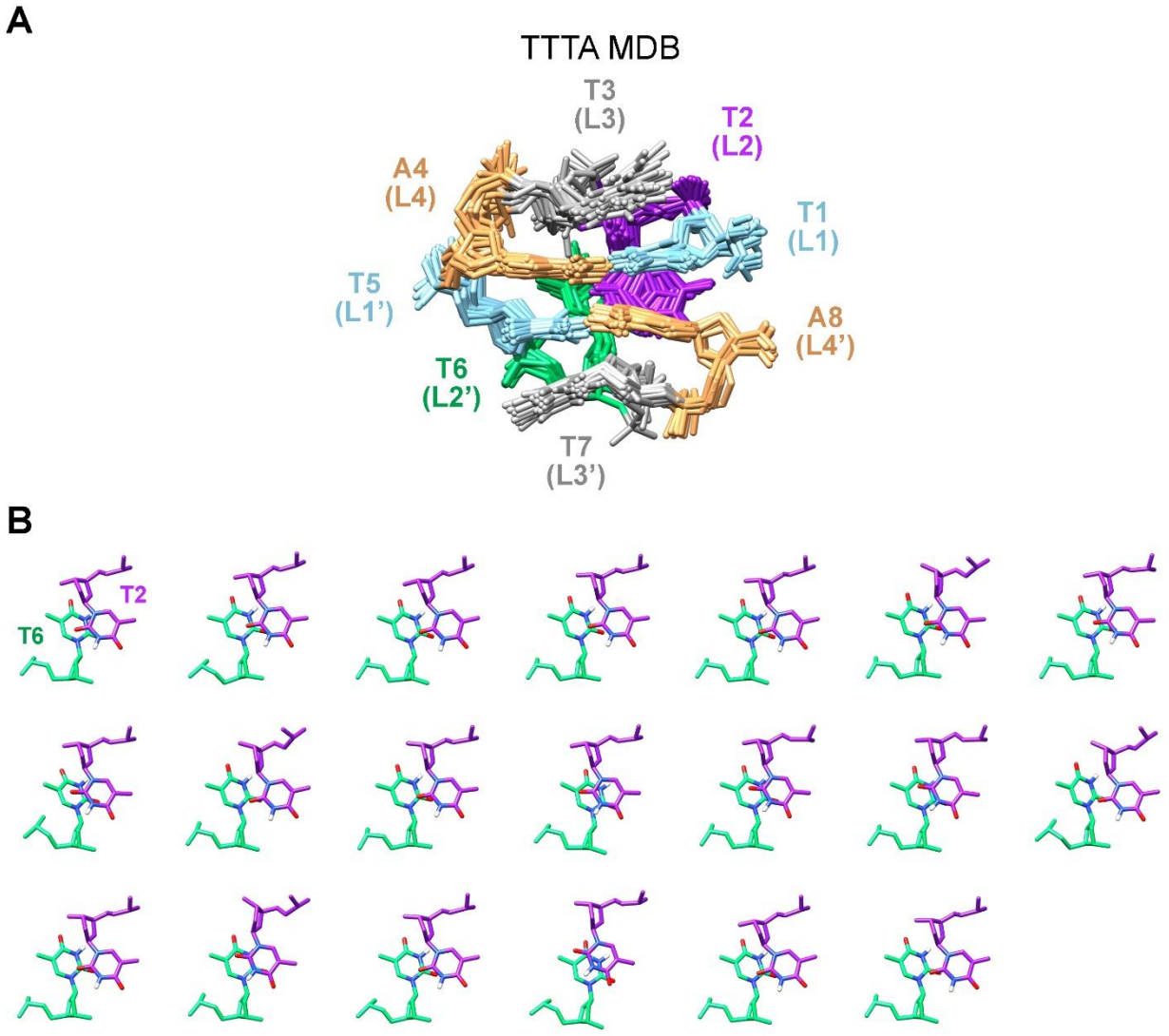

Figure S4. Unusually downfield ^{31}P and H6/H7 signals of L2 and L2' residues support the formation of MDB structures by the new CTTG_X, CCTG_X and TTTA_X sequences, respectively. Similar downfield shifted ^{31}P and ^{1}H signals have been reported for the known CTTG, CCTG and TTTA MDBs, respectively.[9-11] Spectra shown here were acquired at 0 °C.

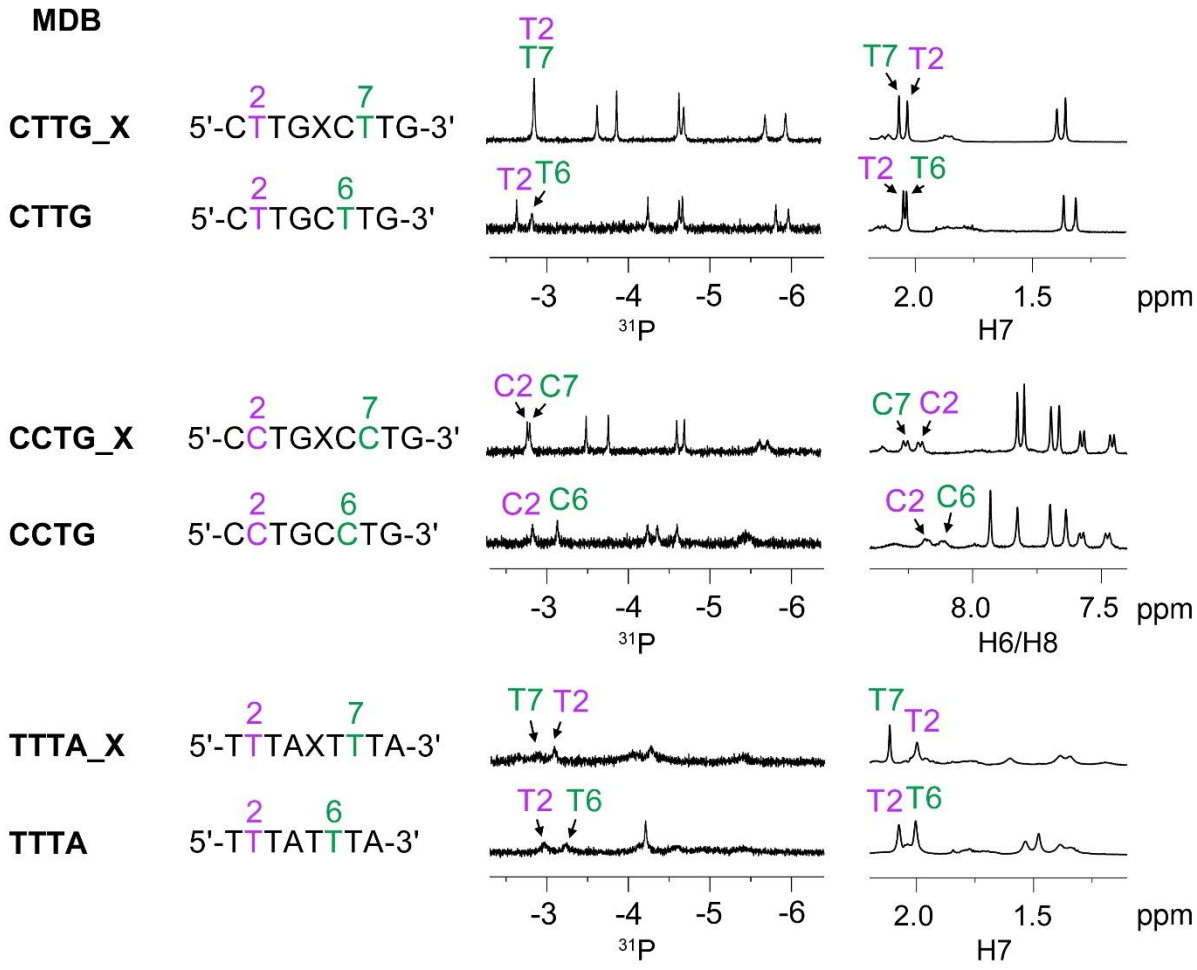

Figure S5. 1D NOE difference spectrum of TTTA_X upon selectively saturating T1 H3 at ~13.5 ppm using excitation sculpting pulse sequence for water suppression (top), and the reference spectrum without saturation acquired using jump-return pulse sequence for water suppression (bottom). In the 1D NOE difference spectrum, appearance of 1D NOEs on A4 H2 and A4 H8 suggests that T1-A4 undergoes exchange between Watson-Crick and Hoogsteen pairing modes. The spectra were acquired at 10 °C.

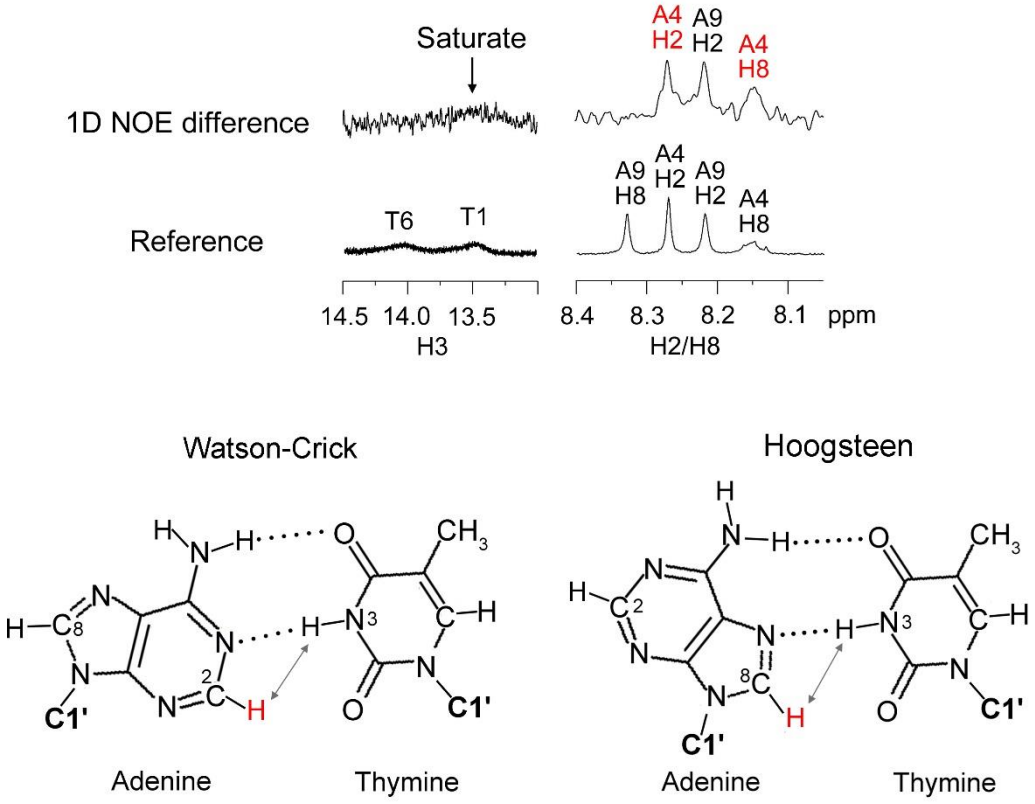

Figure S6. In the CTTG_X MDB (PDB ID: 6M6J), (A) C1-G4 and C6-G9 form Watson-Crick loop-closing base pairs, as supported by the NOEs of C1 H41/H42-G4 H1 and C6 H41/H42-G9 H1, (B) T2 and T7 adopt a reverse wobble T·T mispair as supported by the NOE of T2 H3-T7 H3, and (C) T3 and T8 stack on C1-G4 and C6-G9, respectively, as suggested by the NOEs of T3 H6-G4 H1 and T8 H6-G9 H1. (D) X5 forms an extrahelical bulge, leaving space for extensive base-base stackings between C1-G4 and C6-G9, as suggested by the NOEs of C1 H5-G9 H8 and C6 H5-G4 H8. (E) 2'-methylene groups of G4, X5 and C6 (purple) form a hydrophobic core. The NOESY spectra in (A) and (C) were acquired at a mixing time of 150 ms at 0 °C. The NOESY spectra in (B) and (D) were acquired at a mixing time of 50 and 200 ms, respectively, at 0 °C.

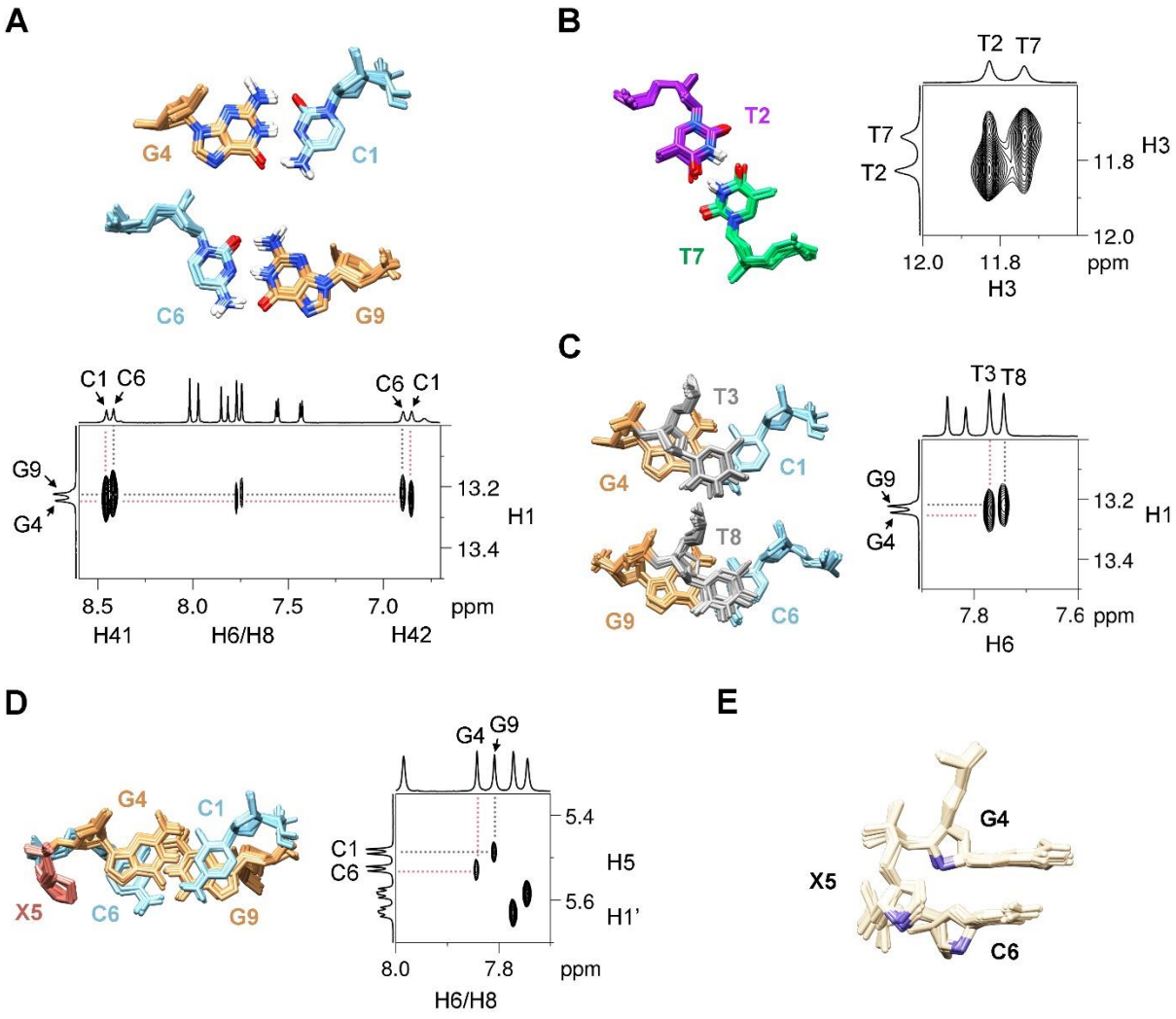

Figure S7. In the CCTG_X MDB (PDB ID: 6M6K), (A) C1-G4 and C6-G9 form Watson-Crick loop-closing base pairs, as supported by the NOEs of C1 H41/H42-G4 H1 and C6 H41/H42-G9 H1, (B) T3 and T8 stack on C1-G4 and C6-G9, respectively, as suggested by the NOEs of T3 H6-G4 H1 and T8 H6-G9 H1, and (C) X5 forms an extrahelical bulge, allowing base-base stackings between C1-G4 and C6-G9, as suggested by the NOEs of C1 H5-G9 H8 and C6 H5-G4 H8. (D) 2'-methylene groups of G4, X5 and C6 (purple) form a hydrophobic core. The NOESY spectra in (A) and (B) were acquired at a mixing time of 200 ms at 0 °C. The NOESY spectrum in (C) was acquired at a mixing time of 300 ms at 0 °C.

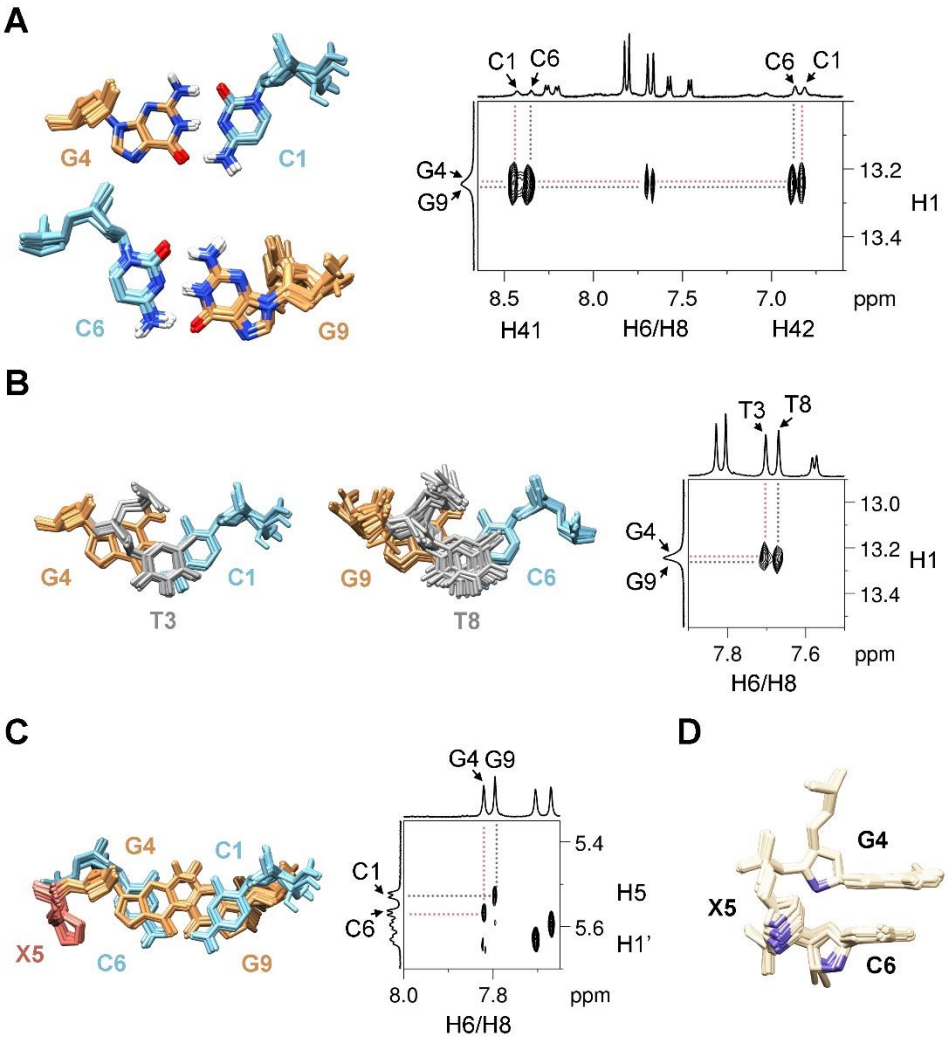

Figure S8. (A) Sequential resonance assignment of the CTTG_X MDB using the NOESY H6/H8-H1' fingerprint region. (B) Assignment of guanine H1 and cytosine H41/H42 signals. The spectra in (A) and (B) were acquired at a mixing time of 200 and 150 ms, respectively, at 0 °C.

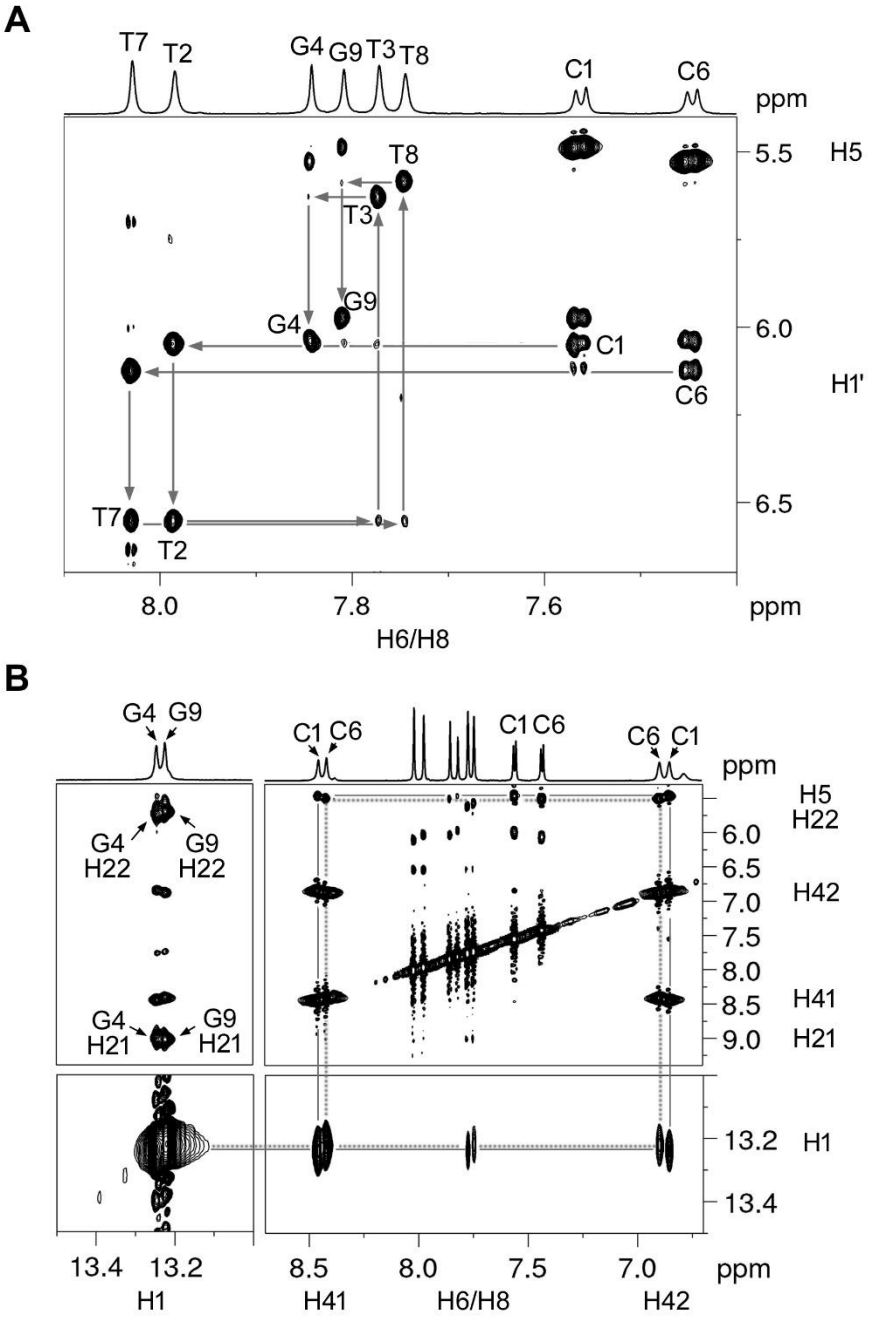

Figure S9. (A) Sequential resonance assignment of the CCTG_X MDB using the NOESY H6/H8-H1' fingerprint region. (B) Assignment of guanine H1 and cytosine H41/H42 signals. The spectra in (A) and (B) were acquired at a mixing time of 300 and 200 ms, respectively, at 0 °C.

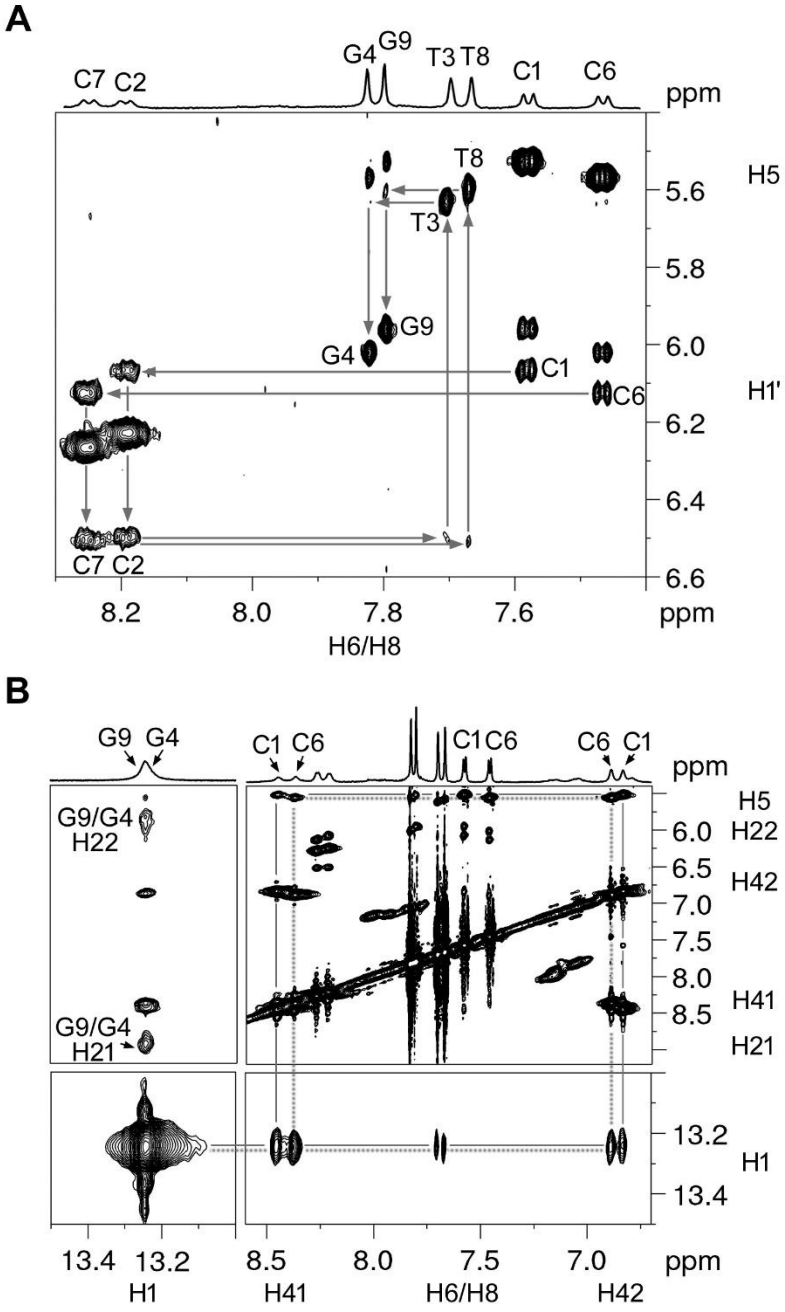

Figure S10. Sequential resonance assignment of the TTTA_X MDB using the NOESY H2/H6/H8-H1' and H2/H6/H8-H2/H6/H8 regions. The spectrum was acquired at a mixing time of 800 ms at 15 °C.

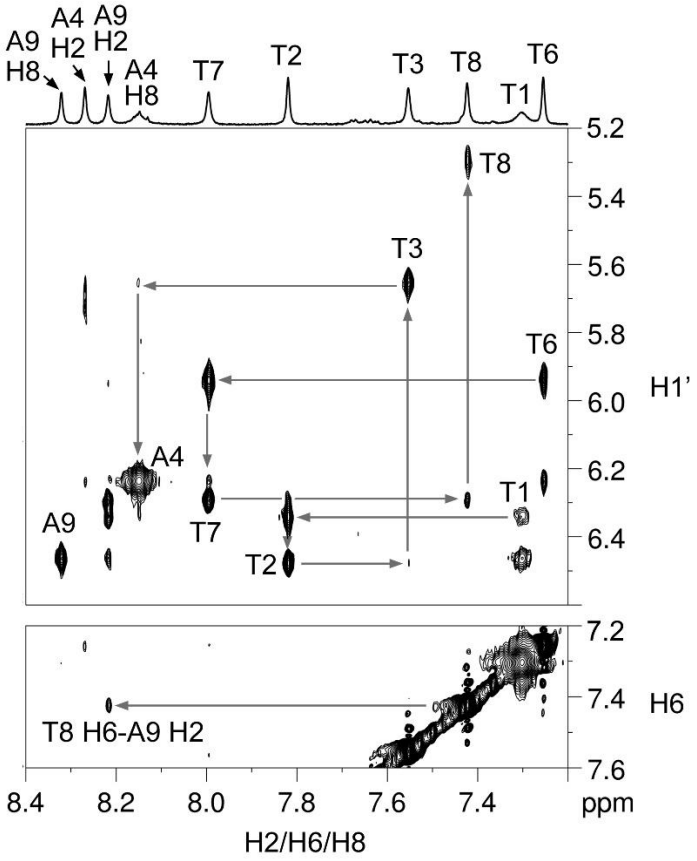

Figure S11. ^{31}P resonance assignment of the CTTG_X MDB using intranucleotide H2'/H2''-H3' and H1'/H1'1/H1'2-H3' TOCSY cross peaks (top and middle) and internucleotide H3'-^{31}P HSQC cross peaks (bottom). The spectra shown here were acquired at 0 °C.

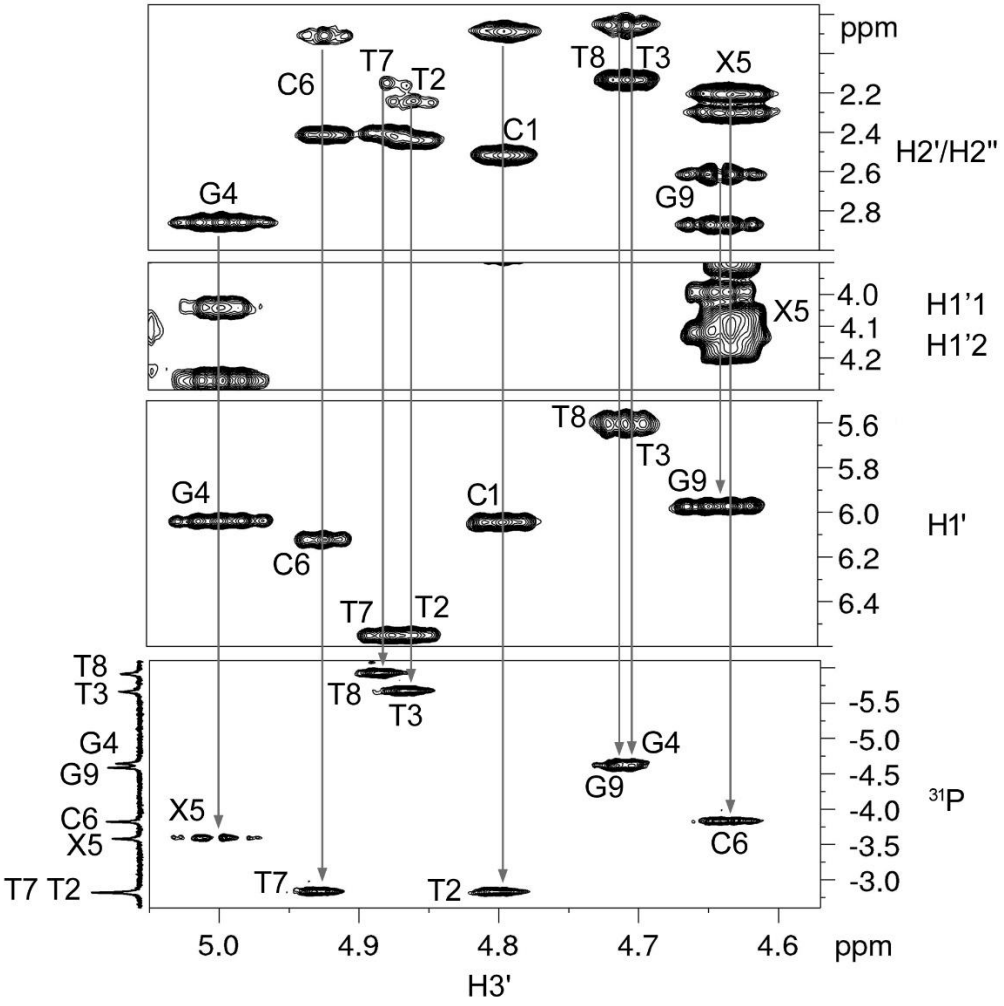

Figure S12. ^{31}P resonance assignment of the CCTG_X MDB using intranucleotide H2'/H2''-H3' and H1'/H1'1/H1'2-H3' TOCSY cross peaks (top and middle) and internucleotide H3'-^{31}P HSQC cross peaks (bottom). The spectra shown here were acquired at 0 °C.

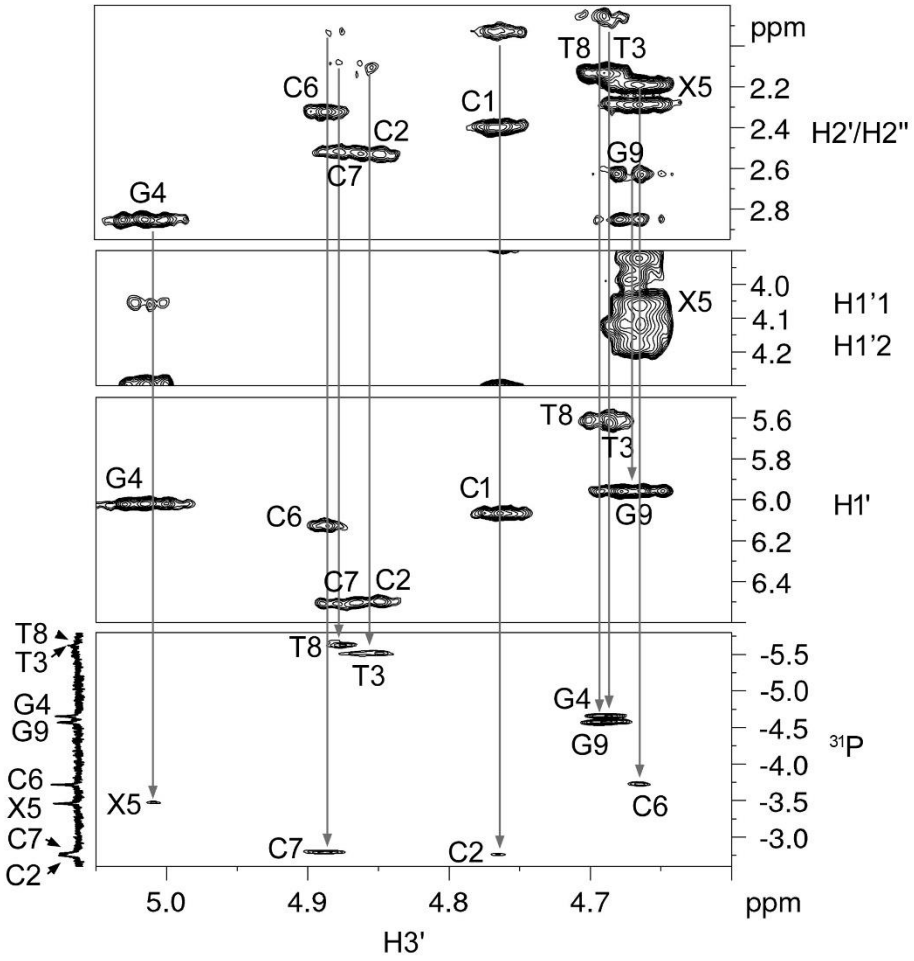

Figure S13. ^{31}P resonance assignment of the TTTA_X MDB using intranucleotide H2'/H2''-H3' and H1'/H1'1/H1'2-H3' TOCSY cross peaks (top and middle) and internucleotide H3'-^{31}P HSQC cross peaks (bottom). The ^{31}P signal of X5 was assigned by excluding other ^{31}P signals. The spectra were acquired at 30 °C.

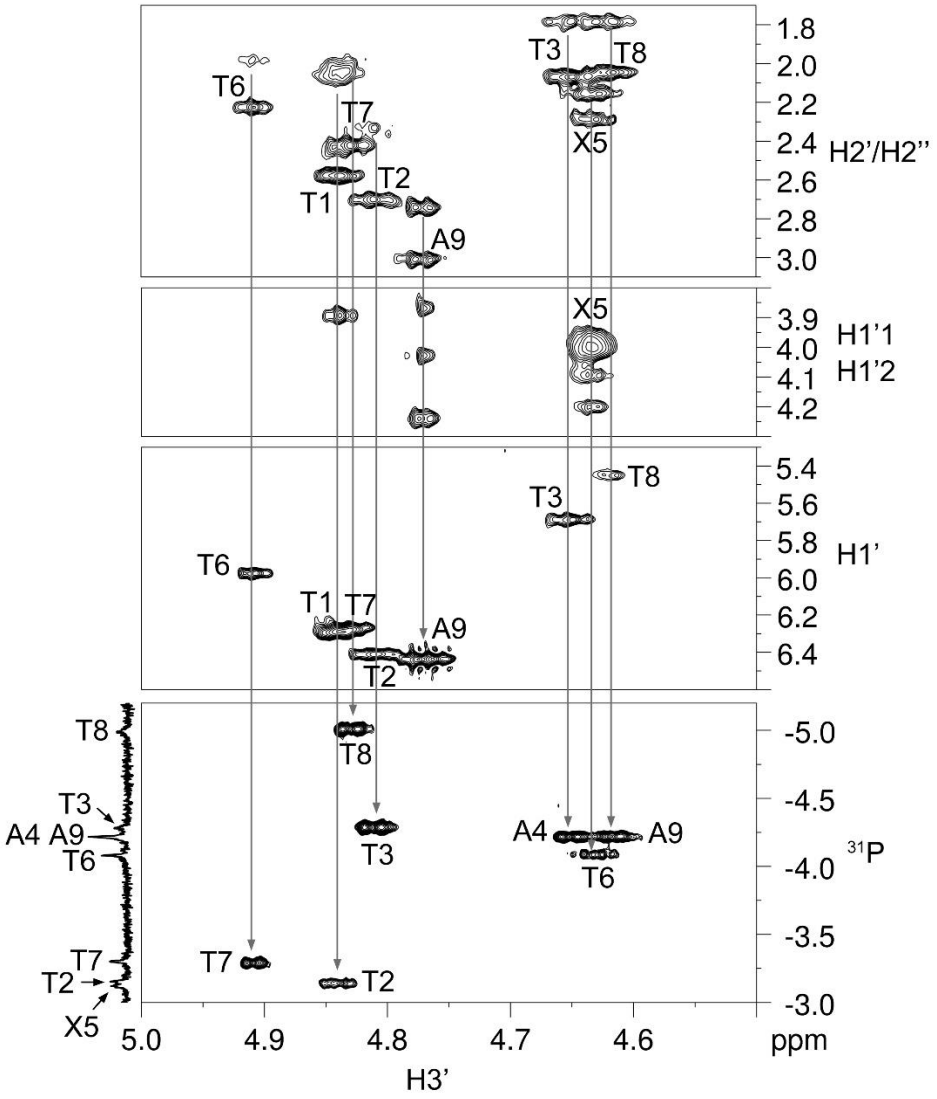

References:

1. K. Stott, J. Stonehouse, J. Keeler, T.-L. Hwang and A. J. Shaka, *J. Am. Chem. Soc.*, 1995, **117**, 4199-4200.
2. P. Plateau and M. Gueron, *J. Am. Chem. Soc.*, 1982, **104**, 7310-7311.
3. M. J. van Dongen, S. S. Wijmenga, R. Eritja, F. Azorin and C. W. Hilbers, *J. Biomol. NMR*, 1996, **8**, 207-212.
4. B. Luy and J. P. Marino, *J. Am. Chem. Soc.*, 2001, **123**, 11306-11307.
5. J. L. Markley, A. Bax, Y. Arata, C. W. Hilbers, R. Kaptein, B. D. Sykes, P. E. Wright and K. Wüthrich, *J. Biomol. NMR*, 1998, **12**, 1-23.
6. S. S. Wijmenga and B. N. M. van Buuren, *Prog. Nucl. Magn. Reson. Spectrosc.*, 1998, **32**, 287-387.
7. K. Wüthrich, *NMR of Proteins and Nucleic Acids*, Wiley, 1986.
8. P. Cuniasse, L. C. Sowers, R. Eritja, B. Kaplan, M. F. Goodman, J. A. Cognet, M. Le Bret, W. Guschlbauer and G. V. Fazakerley, *Biochemistry*, 1989, **28**, 2018-2026.
9. P. Guo and S. L. Lam, *FEBS letters*, 2015, **589**, 1296-1300.
10. P. Guo and S. L. Lam, *FEBS letters*, 2015, **589**, 3058-3063.
11. Y. Liu, P. Guo and S. L. Lam, *J. Phys. Chem. B*, 2017, **121**, 2554-2560.
12. N. J. Greenfield, *Nat Protoc*, 2006, **1**, 2527-2535.
13. W. Saenger, *Principles of Nucleic Acid Structure*, Springer-Verlag, 1984.
14. R. V. Hosur, G. Govil and H. T. Miles, *Magn. Reson. Chem.*, 1988, **26**, 927-944.
15. D. A. Case, T. E. Cheatham, 3rd, T. Darden, H. Gohlke, R. Luo, K. M. Merz, Jr., A. Onufriev, C. Simmerling, B. Wang and R. J. Woods, *J Comput Chem*, 2005, **26**, 1668-1688.
16. Z. Liu, S. Ding, K. Kropachev, L. Jia, S. Amin, S. Broyde and N. E. Geacintov, *PLoS One*, 2015, **10**, e0137124.
17. P. Kraft and K. A. D. Swift, *Perspectives in Flavor and Fragrance Research*, Verlag Helvetica Chimica Acta, Zürich, 2005.
18. M. Zgarbova, J. Sponer, M. Otyepka, T. E. Cheatham, 3rd, R. Galindo-Murillo and P. Jurecka, *J. Chem. Theory Comput.*, 2015, **11**, 5723-5736.
19. D. R. Roe and T. E. Cheatham, *J. Chem. Theory Comput.*, 2013, **9**, 3084-3095.
20. E. F. Pettersen, T. D. Goddard, C. C. Huang, G. S. Couch, D. M. Greenblatt, E. C. Meng and T. E. Ferrin, *J Comput Chem*, 2004, **25**, 1605-1612.
21. A. Onofrio, G. Parisi, G. Punzi, S. Todisco, M. A. Di Noia, F. Bossis, A. Turi, A. De Grassi and C. L. Pierri, *Phys. Chem. Chem. Phys.*, 2014, **16**, 18907-18917.
22. P. Guo and S. L. Lam, *J. Biomol. Struct. Dyn.*, 2020, **38**, 1946-1953.
23. P. Guo and S. L. Lam, *J. Am. Chem. Soc.*, 2016, **138**, 12534-12540.